Modal Analysis of the Ancillary During Femoral Stem Insertion: A Study on Bone Mimicking Phantoms

Anne-Sophie Poudrel, Giuseppe Rosi, Vu-Hieu Nguyen, Guillaume Haiat

1. Title page

Modal analysis of the ancillary during femoral stem insertion: a study on bone mimicking phantoms

Abbreviated title : Femoral stem insertion monitoring by resonance frequency analysis

Anne-Sophie Poudrel[a], Giuseppe Rosi[b], Vu-Hieu Nguyen[b], Guillaume Haiat[a,1]

[a]MSME, CNRS UMR 8208, Univ Paris Est Creteil, Univ Gustave Eiffel, CNRS, 61, Avenue du Général de Gaulle, 94010 Créteil Cedex, France

[b] MSME, CNRS UMR 8208, Univ Paris Est Creteil, Univ Gustave Eiffel, F-94010 Creteil, France

[1] Email : Guillaume.HAIAT@univ-paris-est.fr

2. Abstract and key terms

The femoral stem primary stability achieved by the impaction of an ancillary during its insertion is an important factor of success in cementless surgery. However, surgeons still rely on their proprioception, making the process highly subjective. The use of Experimental Modal Analysis (EMA) without sensor nor probe fixation on the implant or on the bone is a promising non destructive approach to determine the femoral stem stability. The aim of this study is to investigate whether EMA performed directly on the ancillary could be used to monitor the femoral stem insertion into the bone. To do so, a cementless femoral stem was inserted into 10 bone phantoms of human femurs and EMA was carried out on the ancillary using a dedicated impact hammer for each insertion step. Two bending modes could be identified in the frequency range [400-8000] Hz for which the resonance frequency was shown to be sensitive to the insertion step and to the bone-implant interface properties. A significant correlation was obtained between the two modal frequencies and the implant insertion depth (R^2=0.95 ±0.04 and R^2=0.94 ±0.06). This study opens new paths towards the development of noninvasive vibration based evaluation methods to monitor cementless implant insertion.

Keywords: Resonance frequency, Mode shape, Hammer impact testing, Total Hip Arthroplasty, Uncemented implant

3. Introduction

Total Hip Arthroplasty (THA) is one of the most common surgical procedure with more than 1 million THA performed yearly worldwide[35], this number being expected to rise in the next years because of population ageing and because younger patients are now subject to such surgery[23,39]. Currently, both cemented and uncemented technics are used by the surgeons, the first one being the oldest and providing fixation through the cement, which may be advantageous for patients with poor bone quality. Nevertheless, allergic response[41] and shocks due to cement particles detachment[38] may lead to surgery's failure and consequently, pain for patients and important costs for the healthcare system[6]. Therefore, cementless approach[20] was developed consisting of inserting the implant directly in contact with the bone, which fosters bone remodeling at the bone-implant interface and increases the long-term fixation. However, surgical failures also occur because of the difficulty to achieve a good initial fixation, commonly named "primary stability" and which is a crucial determinant of the long-term surgical success[14114]. In particular, the femoral stem (FS) primary stability is achieved by inserting the femoral stem into a slightly undersized bone cavity prepared by the surgeon using adapted rasps. Numerical studies demonstrated that an interference fit between 50 µm to 100 µm is optimal regarding the level of micromotions and the risk of peri-prosthetic fractures[29,43]. Nevertheless, it is difficult to evaluate the remaining dimensions of the cavity in a real configuration as it highly depends on the surgeon reaming. Following bone cavity's preparation, the implant is inserted into the femur through successive hammer impacts realized on the dedicated ancillary. The number and intensity of the impacts realized with the hammer should be optimized in order to find a compromise between:

- maximizing the bone-implant contact ratio to reduce micromotions at the bone-implant interface (BII)[34], while avoiding intraoperative and peri-operative femoral fracture
- achieving a sufficient mechanical fixation, while avoiding excessive stresses

at the BII[10].

As a consequence, it is of great interest to monitor the femoral stem insertion peroperatively and in particular to determine the insertion endpoint to avoid aseptic loosening and peri-operative femoral fracture.

Currently, the per-operative monitoring of the implant insertion is determined by the orthopedic surgeon empirically by visual and hearing assessments[42]. Although the surgeon proprioception remains the gold standard to assess the insertion state quality, such approach is subjective and may lead to errors. Different quantitative techniques are under development to objectively monitor the insertion of cementless implants in the operative room[5]. Most studies consider acoustic and/or vibration methods because imaging systems such as X-ray or MRI create measurement's artefacts near the implant[8]. Moreover, although low dose EOS imaging system is a promising approach to assess the implant position, it remains difficult to be used during the insertion in the operative room.

Acoustic methods have been developed to monitor cementless components insertion in THA by studying the resulting sound produced by hammer impacts performed on the ancillary during the implant insertion process[30]. An *in vivo* study of the femoral stem insertion revealed that the vibro-acoustic behavior is sensitive to the bone-implant system in the frequency range [200-2000] Hz[13]. A convergence-based insertion endpoint criterion, associated to the maximal implant fixation, was developped[12]. Even if this method is contactless, the main limitation is the influence of the environmental noise and the surgeon hammering method on the results.

Vibrational analyses, which are used clinically to assess dental stability[31], have also been applied to orthopedic surgery to monitor either implant insertion[11,36] or to detect acetabular cup loosening[3]. For instance, several studies[17,24,44] used a shaker attached to the implant to retrieve the resonance frequencies of bone-implant system. Pastrav et al.[32] measured FRF at successive insertion stages in the range [0-5000] Hz and they quantified the similarity of two successive FRF graphs using the

Pearson's correlation coefficient as an indicator of the stiffness variation of the bone-implant structure and therefore of the implant stability. Others studies on the acetabular cup considered laser Resonance Frequency Analysis (RFA) where pulsed laser irradiations are applied to the implant and the corresponding vibrations are detected with a laser Doppler vibrometer[21]. It was shown that the resonance frequency between 2 and 6 kHz could predict the pull-down force and therefore measure the implant stability. Complementary approaches focused on using other modal parameters than resonance frequencies to measure the implant fixation, such as the implant corresponding mode shapes[18]. Modal analysis is widely used to determine material properties[15,25] and constitutes a promising approach because it allows to identify the mode shapes, whose spatial dependence is potentially more influenced by local changes in the bone-implant interface than the natural frequency only. A study on the acetabular cup where the sensors were directly fixed on the implant[16] has shown that modal parameters of uncemented implants (resonance frequency and mode shape) depend on the implant fixation into the bone. However, the main drawback of the aforementioned approaches lies in the difficulty of applying it in the clinic either due to i) the modification of the orthopedic implant design with the fixation of sensors, ii) excitation systems that must directly be attached on the implant to measure the FRF or the mode shapes or iii) the complexity of the RFA measurement protocol hardly applicable in the operative room.

Another method was developed by our group based on the analysis of the time dependence of the force applied to the ancillary by a hammer instrumented with a piezoelectric sensor[26]. This method was first applied to assess the acetabular cup primary stability[27] and was validated through the development of numerical models[28]. Then, the same approach was used to monitor the femoral stem insertion *in vitro* in bone phantoms bovine specimens[1] and *ex vivo* in femurs of anatomical subjects[7]. In particular, an indicator based on the time-history of the force signal was used to determine the femoral stem insertion endpoint. The information given by the indicator has been compared to both the surgeon proprioception and to video analysis of the

femoral stem insertion.

The aim of the present study is to provide a method capable of measuring of the bone-implant system status during femoral stem insertion using an instrumented clinical ancillary. The originality is that the method does not require any additional contact with the implant, neither for the excitation source, nor for the response monitoring. The parameters obtained by experimental modal analysis (EMA) with impact excitation performed on the clinical ancillary will be analyzed according to the implant insertion step into bone mimicking phantoms. In order to assess the performances of the method, the results obtained with the EMA will be compared with information retrieved using the instrumented hammer described above[40].

4. Materials and methods

a. Experimental set up for femoral stem insertion

This study was performed using 10 human artificial left femurs (ORTHObones, 3B Scientific, Hamburg, Germany) made of polyurethane foam mimicking trabecular and cortical bone tissues. The implant considered in this study was a cementless femoral stem of size 9 made of titanium alloy (TiAl6Al4V) and coated with hydroxyapatite (CERAFIT R-MIS, Ceraver, Roissy, France). The specimens were prepared similarly as in Tijou et al[40] (see Fig. 1). The implant was inserted by two experimented surgeons by applying successive impacts to the top of a cylindrical-shaped custom-made ancillary (referenced as (5) in Fig. 1) with the same instrumented hammer as in previous studies[1,7,40] (referenced as (1) in Fig. 1). Each impact corresponds to one insertion step noted #*i* and the corresponding force signal $s_i(t)$ was recorded together with the implant relative displacement $E_i = e_i - e_0$ between two successive insertion steps following the procedure used in Tijou et al[40] and described in details in Appendix

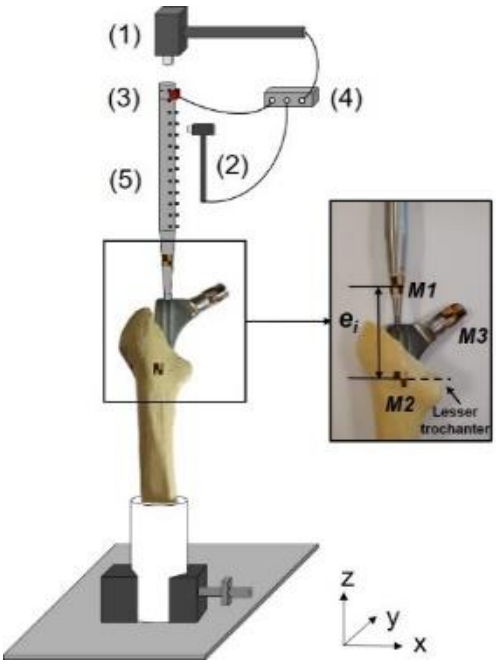

Figure 1 Experimental set up: (1) instrumented hammer; (2) modal hammer; (3) tri-axial accelerometer; (4) Data Acquisition Modulus (DAQ); (5) custom-made ancillary and zoom on the positions of markers #M1. #M2. #M3 and the distance e_i.

A.1&2.

b. Experimental set up for modal analysis

EMA was carried out by analyzing the modal behavior of the ancillary for each implant insertion step #*i*. The EMA set up is described in Fig. 1. The bone phantom specimen was clamped to the vibration table to provide a rigid boundary condition to the system. The ancillary, temporary screwed within the femoral stem to provide a rigid connection between the two parts during the insertion procedure, was equipped with a 3-axial accelerometer (365A01PCB Piezotronics, Depew, NY, USA) located at its top. The axes of the accelerometer were aligned with those of the femoral stem to allow a simple post-processing analysis. A small modal hammer (8204, Brüel & Kjaer, Naerum, Denmark), referenced as (2) in Fig.1, was used as an excitation source. The impact was made with a maximum force lower than 50N in order to make sure that such impact does not modify the implant position. The acceleration signal was recorded by a dedicated data acquisition module (BK Connect, Brüel & Kjaer, Naerum, Denmark) with a sampling rate of 51.2 kHz and a duration of 0.25 s.

Twelve locations equally distributed were defined along the cylindrical part of the ancillary, as shown in Fig. 1. For each implant insertion step #*i*, the ancillary was impacted at each location with the dedicated modal hammer in two perpendicular directions corresponding to the *X* and *Y* directions indicated in Fig. 1, which leads to a total of 24 measurement points for each insertion step #*i*. The impact was repeated five times at each measurement point. As the *X, Y* and *Z* components are stored for each impact, a total of 72 averaged acceleration response signals $\gamma(t)$ and 24 averaged force signals $F(t)$, were recorded, for each insertion step #*i.*

We assumed that the weight of the accelerometer (1 g) does not influence the modal response of the ancillary. Given the low momentum applied with the modal hammer, we assume that the bone-implant system behaves linearly during the modal tests, which was confirmed by an analysis of the coherence functions (not presented in this paper) that provides evidences on the absence of non-linearity or high noise level[9].

c. Experimental protocol

The femoral stem was inserted one time only in each bone phantom specimen except for specimen #7, where it was inserted three times to study the EMA sensitivity to successive insertions. A dedicated iterative experimental protocol illustrated in Fig. 2 was carried out for each insertion step #*i* and for 10 additional impacts after the one corresponding to the optimal insertion end-point that was determined empirically based on the surgeon proprioception. The protocol for the reproducibility evaluation of EMA and the corresponding results on the resonance frequency variation are presented in Appendix A.3.

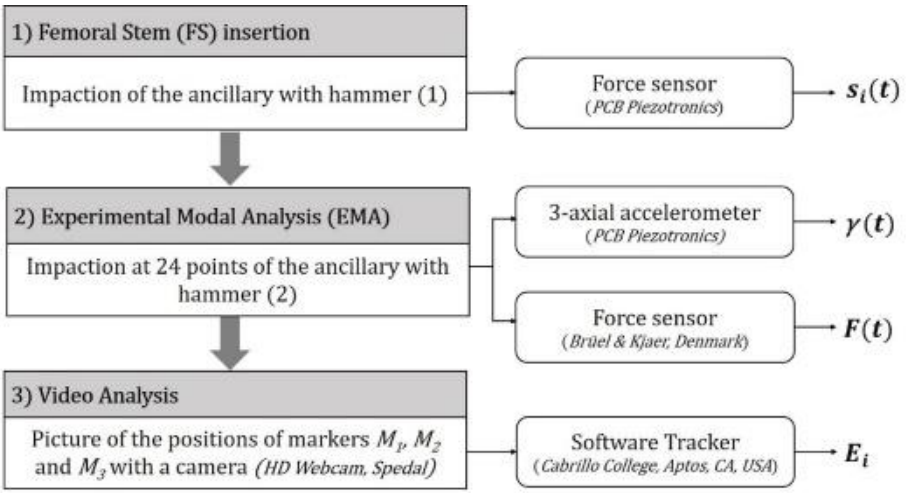

Figure 2 Experimental measurement protocol performed for each implant insertion step #i on all bone phantom specimens.

d. Data analysis

Insertion monitor by the instrumented hammer

The same indicator D_i as developed in previous studies[1,7,40] was calculated from the impact force signal $s_i(t)$, corresponding to the time between the two first peaks of $s_i(t)$ (see Appendix A.1) for each insertion step #*i*.

Modal Analysis and Parameter Estimation

The acceleration signals $\gamma(t)$, as well as the impact forces $F(t)$ recorded by the modal hammer (2), need to be processed in order to extract the modal parameters, namely the modal (or resonance) frequencies, the mode shapes and the modal damping. Due to the large number of datasets, the modal parameter estimation was performed using a dedicated software for modal analysis (BK Connect, Brüel & Kjaer, Naerum, Denmark) following the method described below. First, an exponential weighting window was applied for both the force (input) and the acceleration (output) signals. Then, the Fast Fourier Transforms (FFTs) of all acceleration and force signals were computed and were denoted $\hat{\gamma}(\omega)$ and $\hat{F}(\omega)$. Eventually, all the Frequency Response Functions (FRFs), noted $h(\omega)$ were determined as follows[9]:

$$h(\omega) = \frac{\hat{\gamma}(\omega)}{\hat{F}(\omega)} \quad (1)$$

For each insertion step #*i*, 72 FRFs $h(\omega)$ were calculated with Eq. (1), considering the FFTs $\hat{\gamma}(\omega)$ of the 72 time accelerations signals $\gamma(t)$ recorded for each direction *X, Y, Z* and for each one of the 24 measurement points. A multidegree-of-freedom (MDOF) modal analysis extraction method, called the Rational Fraction Polynomial (RFP) algorithm, was used to estimate the corresponding modal parameters. This method[37], provides a curve-fitting to all FRFs corresponding to the same insertion step #*i*, considering the problem as a linear set of equations defined by an analytical fraction FRF formulation. Then, the MDOF method consists of determining for each insertion step #*i* the resonance frequencies f^n and the modal dampings ζ^n so that the reconstructed transfer function, noted $H(\omega)$, approaches $h(\omega)$ within the frequency range $f \in$[400-8000] Hz, determined considering the modal hammer bandwidth and the results of Qi et al[36] about the optimal frequency range to study femoral stem connection with the host bone.

The mode shapes vectors $\underline{\phi_i^n}$, for $n \in [0, N_i]$ were retrieved from $h(\omega)$ at the resonance $f_i = f^n$ obtained at each measurement point. Note that the number of modes N_i which could be identified, can vary as a function of #*i,* since the mechanical system evolves during the insertion procedure.

Mode Shape Tracking

The Modal Assurance Criterion (MAC) was used to track the modes of the ancillary throughout the insertion process. The MAC is defined as a scalar providing a measure of consistency between two modal vectors $\underline{\phi_1}$ and $\underline{\phi_2}$ and is defined as follows[2]:

$$MAC(\underline{\phi_1}, \underline{\phi_2}) = \frac{\underline{\phi_1^T}\,\underline{\phi_2^*}}{\underline{\phi_1^T}\,\underline{\phi_1^*}\,\underline{\phi_2^T}\,\underline{\phi_2^*}} \tag{2}$$

where $\underline{\phi^T}$ is the transpose of $\underline{\phi}$ and of $\underline{\phi^*}$ is the complex conjugate of $\underline{\phi}$. Equation 2 is a normalized Hermitian inner product between two modal vectors. A MAC value close to 1 indicates a high degree of collinearity between the two mode shapes $\underline{\phi_1}$ and $\underline{\phi_2}$, while a MAC value close to 0 means that the two modes $\underline{\phi_1}$ and $\underline{\phi_2}$ are nearly orthogonal. By applying this concept to a set of modes from the same insertion step #*i*, one obtains a symmetric matrix *A* which is expected to be close to an identity matrix and which can therefore be used as a quality assessment for the modal extraction. Then the matrix coefficients are defined for *p, q* ∈ [0,N_i] by :

$$A_{pq} = MAC(\underline{\phi_p}, \underline{\phi_q}). \tag{3}$$

In this study, the MAC is used to identify and track one or several specific modes from one insertion step #*i* to another insertion step #*j.* Since the boundary conditions of the ancillary varies with the implant insertion step, the mode shape $\underline{\phi_i^n}$ may slightly evolve between different insertion steps #*i*, especially in the first insertion steps. Therefore, the coefficients $A_{ij}^n = MAC\left(\underline{\phi_i^n}, \underline{\phi_j^n}\right)$ with $(i \neq j)$ are expected to be different from 1. Furthermore, based on Henys and Capek[16], we assume that a MAC value A_{ij}^n higher to 0.75 provides the mode tracking from the successive insertions steps #*i* and #*j* by ensuring that all modes are uniquely paired. Eventually, for certain modes, the coefficients A_{ij}^n were calculated for all the insertions steps *i≠j* leading to the evolution of a specific mode shape $\underline{\phi^n}$ throughout the insertion procedure.

Parameter evaluation to monitor femoral stem insertion

Our previous studies showed that the indicator D_i could be used to estimate the implant insertion endpoint, with a significant correlation with the surgeon proprioception[1,7,40], for which the corresponding insertion step was noted N_{surg}. In the present study, the variation of the modal frequency f^n obtained with the EMA was compared to the variation of the indicator D_i as a function of the impact number *#i.* The convergence of both D_i and f^n was characterized by two thresholds defined empirically as the lowest impact number $i = N_f$ for which:

$$D_i < \overline{D} + 2 \times D_{std} \tag{4a}$$

And

$$f_i^n > \overline{f^n} - 2 \times f_{std}^n \tag{4b}$$

where $\overline{f^n}$, f_{std}^n, $\overline{D}$ and and D_{std} correspond to the mean and standard deviation values of the modal frequency n and the indicator D for the 6 (respectively 10) last impacts. The choice of the number of impacts considered will be discussed in Sec. 4.

5. Results

a. Mode shape features

Three bending modes of the ancillary could be identified in the frequency range [400-8000] Hz for all bone mimicking specimens and all insertion steps. The total number of insertion steps varies between 15 to 18 according to the specimen. The modal characteristics (given by the resonance frequency and the shape curvature) were obtained by the RFP method. A representation of the deformed shape of these three bending modes is shown in Fig. 3a. This illustration is obtained from the FRF at the resonance frequency f^n, retrieved at each measurement point for a specific insertion step $i = 14$ corresponding to a step at the end of femoral stem insertion into the bone phantom *#3*. The magnitude of the arrows drawn at each measurement point in the three orthogonal directions *X, Y, Z* is proportional to the mode shape calculated in each direction. The deformed shape is compared to the undeformed shape of the cylindrical part of the ancillary, represented by the thin vertical line in the middle of

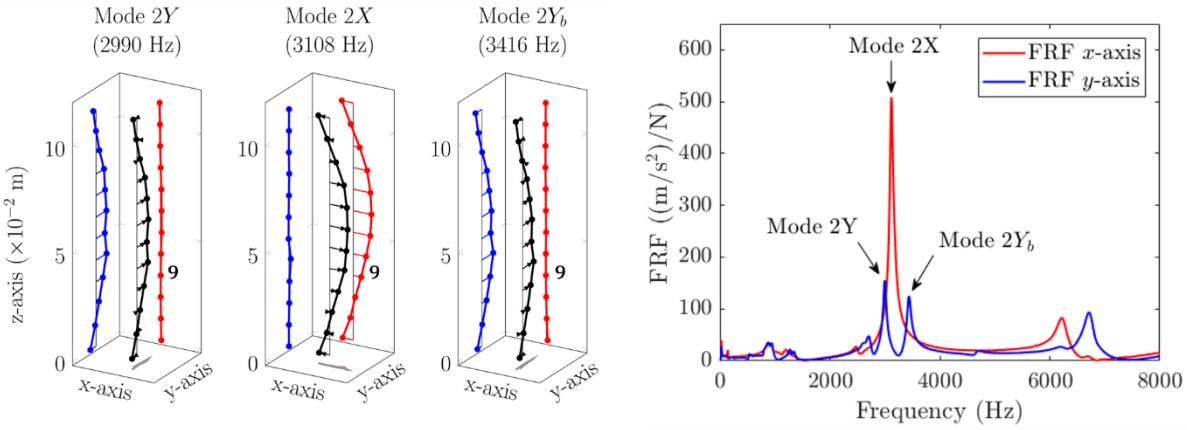

Figure 3 a) Description of three mode shapes of the ancillary (represented by black lines) in the frequency range [400-8000] Hz at femoral stem insertion step #15 in bone phantom #3. The points correspond to the measurements points and the arrows represent the ancillary response function and b) Frequency response functions measured for the same configuration by the accelerometer for an impact on the ancillary with the modal hammer in X (blue curve) and Y (red curve) directions at measurement point 9.

the boxes. For ease of reading, the notation of the modes is based on the number of nodes on the ancillary and on the plane of vibration, defined in Fig. 1. Among the three modes shown in Fig. 3, the modes $2Y$ and $2Y_b$ oscillate in the *YZ* plane, while mode $2X$ oscillates in the *XZ* plane. The number of nodes is in all cases equal to two for the three modes considered herein. Even if the shapes of modes $2Y$ and $2Y_b$ look similar (bending modes with two nodes), they are identified as two distinct modes since they have two different resonance frequencies f_{2Y} and f_{2Y_b}, as shown in Table 1. Moreover, an example of two frequency response functions corresponding to the configuration of Fig. 3a and recorded for two modal hammer impacts in the *X* and *Y* directions at measurement point 9 from the top of the ancillary (see Fig. 3a) is shown in Fig. 3b The two modes $2Y$ and $2Y_b$ are visible on the FRF recorded in *Y* direction (red curve) with peaks around 2990 Hz and 3416 Hz respectively, whereas the peak of mode $2X$ appears on the FRF recorded in *X* direction at 3108 Hz. Furthermore, the modes $2Y$ and $2Y_b$ may be distinguished by the vibration of the femoral stem, which is not measured in this study. This point will be detailed in Sec. 4. In what follows, it was chosen to not show the data corresponding to mode $2X$ since both the mode shape and the resonance frequency f_{2X} do not change between the different insertion steps (see Table 2).

TABLE 1: Values of the thresholds defined for the indicator D_i and for the modal frequency f_{2Y} and f_{2Y_b} for all bone phantom specimens

Specimen	1	2	3	4	5	6	7	8	9	10	Mean	SD
D_i (ms)	0.70	0.58	0.50	0.57	0.73	0.67	0.71	0.51	0.47	0.50	0.59	0.10
f_{2Y} (Hz)	2864	2837	2990	3012	2899	2678	2974	2860	2790	2842	2875	101
f_{2Y_b}(Hz)	3419	3463	3416	3593	3450	3341	3718	3609	3505	3447	3496	112

TABLE 2: Mean frequency f_{2X} and standard deviation $\sigma_{f_{2X}}$ of mode $2X$ over all insertion steps #*i* for all bone phantom specimens

Specimen	1	2	3	4	5	6	7	8	9	10	Mean	SD
f_{2X} (Hz)	3131	3153	3108	3189	3089	3044	3126	3164	3142	3147	3129	41
$\sigma_{f_{2X}}$ (Hz)	15	13	26	26	26	66	55	32	44	13	-	-

b. Modes tracking

The Modal Assurance Criterion (MAC) is employed to track the mode shapes throughout the implant insertion procedure. The results in Fig. 4a and Fig. 4c show coefficient values A_{ij} between 0.6 and 1 for all the compared insertion steps which reveals a change of the shape of both ancillary's modes $2Y$ and $2Y_b$ throughout the implant insertion procedure. The figure was truncated after the 15th step in order to

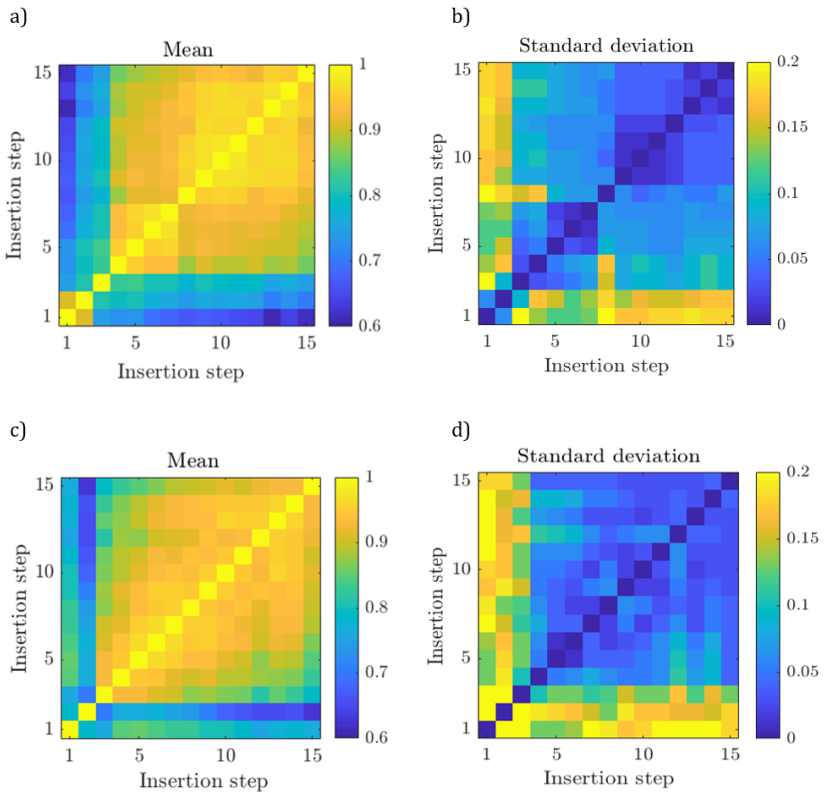

Figure 4 Matrix representation of the mean and standard deviation of the MAC coefficients A_{ij} over all the specimens calculated between two modal vectors measured at insertion step #i (x-axis) and #j (y-axis) for mode $2Y$ (a)(b) and mode $2Y_b$ (c)(d). The colorscale codes the averaged and the standard deviation values of A_{ij} over the specimens.

take into account all the specimens in the matrix representation, the total number of insertion steps varying between 15 and 18 over the specimens. As expected, lower coefficient values are obtained for the initial insertion steps which can be explained by the significant modification of the implant position into the bone phantom at the

beginning of the insertion procedure, which influence the mode's shapes. From a specific insertion step (i=4 for mode $2Y$ and i=3 for mode $2Y_b$), the mode shapes do not change compared to the beginning of insertion which is illustrated by higher A_{ij} values, which are closed to 1. Moreover, as expected, the standard deviations associated to the averaged values of A_{ij} are lower for the final insertion steps than for the initial ones, since at the beginning of insertion the implant displacement is higher than at the end, leading to more important discrepancies between the specimens (see Fig. 4b and Fig. 4d).

c. Femoral stem insertion monitoring

An example of the impact force time signal $s_i(t)$ and the corresponding values of the indicator D_i is presented in Appendix A.4. Figure 5 shows an example of the evolution of the modal frequencies f_{2Y} and f_{2Y_b} and the indicator D_i with the insertion step #*i* of femoral stem insertion in bone phantom #*3*, for which the total number of insertion step is equal to 15. The results first show an increase of the modal frequencies f_{2Y}

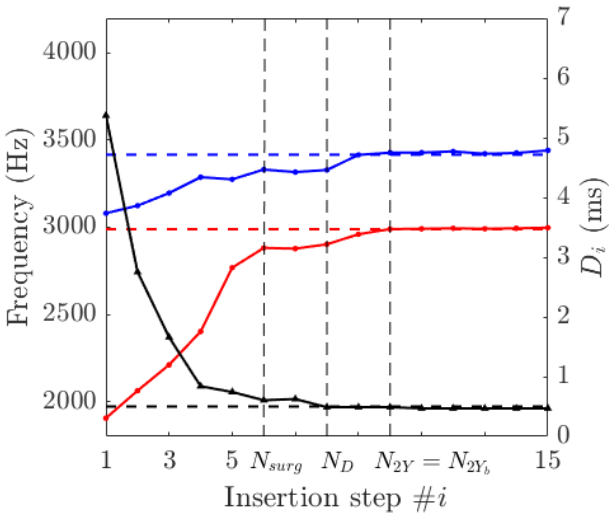

Figure 5 Evolution of resonance frequencies f_{2Y} (in red), f_{2Y_b} (in blue) and the indicator D_i (black) as a function of the implant insertion step #i for bone phantom specimen #3. The black (respectively red and blue) dashed line represents the con- vergence threshold of D_i (respectively mode $2Y$ and $2Y_b$). The insertion steps N_{surg}, N_D, N_{2Y} and N_{2Y_b} corresponding to the feature convergence are indicated on the x-axis.

and f_{2Y_b} and a decrease of D_i as a function of the insertion step #*i* until each indicator stabilizes.

TABLE 3: Gap of insertion step between convergence of D_i and modal frequencies f_{2Y} and f_{2Y_b}

Specimen	1	2	3	4	5	6	7	8	9	10	Mean	SD
$N_{2Y} - N_D$	1	0	2	3	3	4	4	4	3	6	**3**	**1.7**
$N_{2Y_b} - N_D$	3	5	2	3	3	1	5	4	3	3	**3.2**	**1.2**
$N_{2Y} - N_{2Y_b}$	2	5	0	0	0	-3	1	0	0	0	**0.2**	**2.3**
$N_D - N_{surg}$	-1	1	2	1	1	-1	0	0	0	-1	**0.2**	**1.0**
$N_{2Y} - N_{surg}$	0	1	4	4	4	3	4	4	3	5	**3.2**	**1.5**
$N_{2Y_b} - N_{surg}$	2	6	4	4	4	0	5	4	3	2	**3.4**	**1.7**

TABLE 4: Correlation coefficients R^2 between the resonance frequencies f_{2Y}, f_{2Y_b} and E_i into the bone for all bone phantom specimens

Specimen	1	2	3	4	5	6	7	8	9	1	Mean	SD
Mode $2Y$	0.86	0.99	0.98	0.94	0.98	0.97	0.98	0.91	0.94	0.98	**0.95**	**0.04**
Mode $2Y_b$	0.87	0.99	0.98	0.99	0.89	0.96	0.90	0.98	0.81	0.99	**0.94**	**0.06**

The threshold's values for f_{2Y}, f_{2Y_b} and D_i, represented by the dashed-lines in Fig. 5, are presented in Table 1 for all bone phantom specimens. Although the same behavior throughout the insertion procedure can be observed over the different specimens for each type of indicator (D_i, f_{2Y} and f_{2Y_b}), the threshold's values vary according to the specimen, which will be discussed in Sec. 4. For all threshold defined for the indicator D_i and for the modal frequencies f_{2Y} and f_{2Y_b}, the corresponding

insertion step number N_D, N_{2Y} and N_{2Y_b} were defined and are indicated in Fig. 5 by the vertical lines (in black, red and blue, respectively). For the specimen *#3*, $N_{surg} = 6$, $N_D = 8$ and $N_{2Y} = N_{2Y_b} = 10$. The differences of the insertion endpoint N_{surg}, N_D, N_{2Y} and N_{2Y_b} are indicated in Table 3 for all bone phantom specimens. Similarly as in the study of Tijou et al[40], the surgeon's decision is in good agreement with the convergence of D_i, with an insertion step's gap of 0.2 ±1 in average over the specimens. Moreover, in average, the convergence steps of the resonance frequencies are reached 3 steps after the convergence of the indicator D_i.

Figure 6 shows the variation of the modal frequencies f_{2Y} and f_{2Y_b} as a function of the implant relative displacement E_i for bone phantom specimen *#3*, together with a linear regression analysis. As shown in Table 4, a significant correlation was obtained between f_{2Y} (respectively f_{2Y_b}) and E_i for all bone phantom specimens, with an average correlation coefficient $R^2 = 0.95 \pm 0.04$ (respectively $R^2 = 0.94 \pm 0.06$). The data retrieved for the insertion step after which the variation of the displacement E_i is

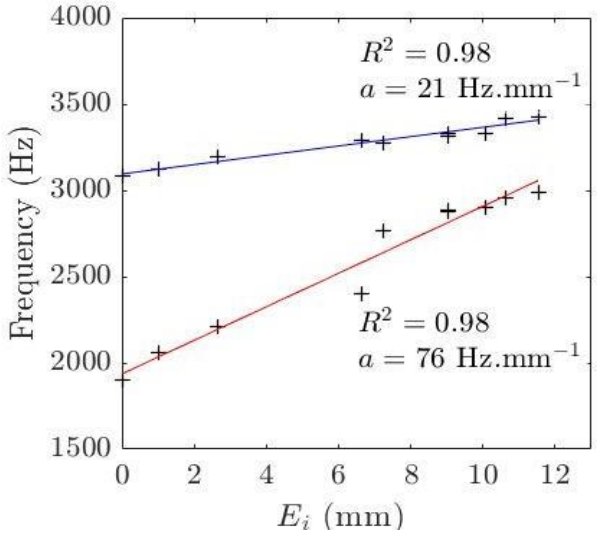

Figure 6 Relationship between modal frequency evolution of modes 2Y (f_{2Y}) and 2Y$_b$ (f_{2Y_b}) of the ancillary and the implant relative insertion depth E_i together with the corresponding linear regression analysis (red and blue lines, respectively) and values of the slopes a into the bone phantom specimen #3.

inferiori to 5% of the total displacement were removed for the analysis since the aim is to evaluate the relation between the variation of modal frequencies f_{2Y} and f_{2Y_b} and the femoral stem displacement E_i during insertion.

d. Sensitivity of EMA to successive implant insertions

The same behavior as the one described previously is obtained for the three successive insertions with an increase of the modal frequencies f_{2Y} and f_{2Y_b} (respectively a decrease of D_i) until the values reach a ”plateau”. However, Figure 7 shows that all parameters reach the plateau faster for the second and third insertions compared to the first one. This result may be explained by wear phenomena in the bone cavity after the first insertion procedure, which will be detailed in Sec. 4.

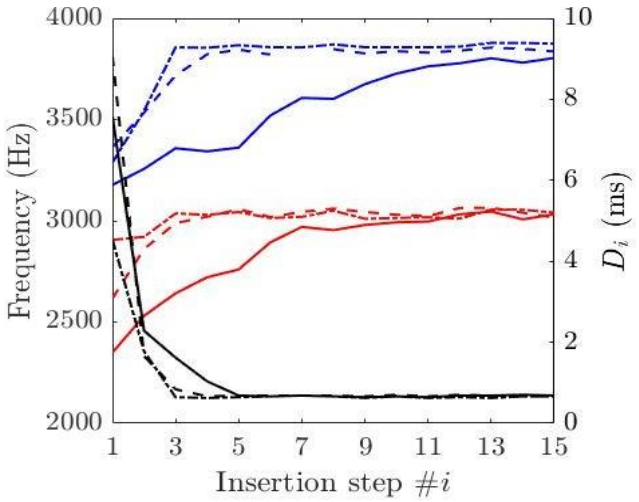

Figure 7 Variation of D_i (black lines), and the modal frequencies f_{2Y} (red lines) and f_{2Y_b} (blue lines) as a function of the insertion step #i for three successive full insertion procedures of the femoral stem into the same bone phantom specimen #7. The solid (respectively dashed and point-dashed) line represents the variation of the parameters for the first (respectively second and third) implant insertion procedure.

6. Discussion

This work aims to investigate whether EMA can be employed to monitor the femoral stem insertion into the host bone. For this purpose, a new protocol was set up where EMA is performed on the ancillary and not directly on the implant nor the bone, which allows to consider such approach to be used in clinical conditions in the future. In this work, the sensitivity of the resonance frequencies and the corresponding mode shapes in the frequency range [400-8000] Hz was investigated throughout the insertion procedure and the results were compared to another monitoring method developed by our group based on the analysis of the force used to insert the implant[40].

a. Sensitivity of the modal parameters to the implant insertion state

Three bending modes of the ancillary could be identified at every step of the femoral stem insertion for all bone phantom specimens (see Fig. 3). The corresponding resonance frequencies f_{2Y} and f_{2Y_b} vary as a function of the insertion step *#i.* The evolution of the indicator D_i presented in Appendix A.4 and Fig. 5 is consistent with previous studies of our group[1,7,40], which allows to compare the results obtained using the method developed herein with previous results. A good qualitative agreement was found between the two methods for implant insertion monitoring (see Fig. 5): the increasing behavior of f_{2Y} and f_{2Y_b} is consistent with the decreasing one of the time indicator D_i. However, Figure 5 and Table 3 show that the resonance frequencies reach a plateau in average three insertion steps after D_i, which show that modal frequencies carries another information on the bone-implant characteristics during the insertion procedure, which is not given by the indicator D_i. Moreover, the significant correlation between the resonance frequencies f_{2Y} and f_{2Y_b} and the femoral stem relative displacement E_i into the bone phantom may be explained by an increase of the stiffness of the bone-implant system[13,18].

In a previous study carried out with bone phantom specimens, a unique threshold for D_i was defined empirically and was equal to 0.53 ms[40]. However, the objectives and the experimental configuration of the present work differ from Tijou et al[40] since only

one size was tested and only one femoral stem insertion was realized for each bone phantom specimen, contrarily to the previous study where successive implant insertions were repeated with the same specimen. Therefore, even if the choice of a unique threshold equal to 0.53 ms would have been consistent considering the standard deviation of D_i equal to 0.10 ms, it would have led to an underestimation of the insertion step N_D for six specimens (see Table 1). Consequently another definition of the convergence threshold of D_i given by Eq. (4a) was used where the threshold varies according to the bone phantom specimen which improves the correlation between N_D and the actual convergence of the indicator D_i.

b. Sensitivity of the modal parameters to the bone cavity properties

After the experiments, the bone phantom specimens and in particular the cavity, was visually checked and any crack nor defect was detected. Even if the same behavior was obtained for the evolution of f_{2Y} and f_{2Y_b} throughout the insertion procedure for all bone phantom specimens, the frequency's convergence thresholds of mode $2Y$ and $2Y_b$ defined by Eq. (4b) vary according to the specimen (see Table 1). Such variations may be explained by differences in the bone phantom geometry since the cavity was reamed manually by the surgeon. The sensitivity of EMA to changes of the cavity properties was also studied by repeating the femoral stem insertion three times in the same bone specimen. A faster increase of the modal frequencies (a faster decrease of the indicator D_i, respectively) was obtained for the second and the third insertion procedure than for the first one (see Fig. 7). During the first insertion procedure, trabecular bone at the bone-implant interface may have been slightly damaged due do the frictional forces at the bone-implant interface[19]. Therefore, the cavity may have been enlarged, especially between the first insertion and the following ones which could explain a faster increase of the resonance frequency because the implant relative displacement is higher for equivalent insertion force.

c. Limitations

A first limitation of the study lies in the large measurement time required to retrieve

the full mode's shapes which limits its application in the operating room. Therefore, to be applicable in clinic, it would be interesting to assess the resonance frequencies from the FRF retrieved at a specific location of the ancillary. This optimal location can be determined with respect to the mode's shapes identified in this study and in particular, far from the nodes. The important time needed to perform the measurements comes from the choice of the number of measurement points equal to twelve and leading to a spatial resolution of the mode shape of 10 mm, which was determined in order to optimize both the duration of the measurement protocol and the accuracy of the modal parameters estimation. Moreover, it was not possible to impact the ancillary according to the *Z* direction except on its top due to the configuration. Therefore, the construction of the mode shape is based only on the excitation and acceleration measurements in the *X* and *Y* directions and it was assumed to consider the ancillary as a 1D system represented by a vertical line. Note that a better FRF estimation method such as the one proposed by Kim et al[22] could have been used to minimize the noise from the input and output signals.

A second limitation is associated to the fact that the ancillary must be screwed within the femoral stem in order to provide a rigid connection between both parts and to enable EMA to be sensitive to the changes at the bone-implant interface without sensor fixation or solicitation on the bone nor the implant. This rigid fixation requires to design an ancillary that is screwed in the FS implant, which is not always possible with all implants. Note that an accelerometer could be fixed on the implant or the bone to retrieve the mode shapes of the whole system, similarly as what was done in Henys and Capek[16] but such approach would be more difficult to transpose to the operative room because of sterilization and biocompatibility issues.

A third limitation lies in the bone model and the experimental configuration which have several drawbacks concerning the material properties, the specimen's geometry and configuration compared to a clinical situation. First, the use of bone mimicking phantoms instead of actual human femurs, which is likely to modify the mechanical response of the bone-implant system because of the difference in terms of bone

properties and presence of surrounding soft tissues. In particular, it is expected that the damping of the peaks at resonance would be more important in real clinic conditions because of both the composite bone properties and the rigid connection of the current in vitro configuration. Moreover, although considering half of the femur is a commonly employed configuration when studying femoral stem insertion monitoring[29,33,40], such configuration is likely to affect the values of the resonance frequency, which is why the same length was considered for all specimen. Also, the samples were rigidly attached is also likely to affect the results but we also considered the same configuration for all specimen. Note that in a previous study carried out for the acetabular cup[4], we showed that the results did not depend on the thickness of soft tissues located around the samples. Therefore, the results cannot be directly translated to the clinical practice and the quantitative values obtained in the study should be then understood as a demonstration of the methodology. It would be of great interest to further test the method on anatomical subject to be closer to real case clinical condition and retrieve quantitative data needed for developing of a future medical device.

Eventually, a fourth limitation lies in the post-processing analysis and the determination of the thresholds calculated *a posteriori*, which may be a limiting factor in the clinic since non-necessary impacts applied by the surgeon must be avoided. To overcome this issue predictive methods should be set up in order to provide real-time information about the thresholds to the surgeon. For that purpose, the use of larger bone datasets and the development of numerical models would be relevant to study the influence of biomechanical and geometrical parameters as the trabecular bone Young's modulus or the interference fit corresponding to the size's difference between the bone cavity and the implant.

d. Development of a future medical device

Being able to objectively monitor and follow implant insertion per-operatively is likely to support the surgeon in the decisions made during the impaction stage, especially

in the last stages of insertion. Although the present methodology cannot be directly applicable in clinical conditions because of the required time of measurement, our approach could be used in the future to provide a decision-support system to the surgeon-independent using frequency measurements obtained following the same method.

From the practical point of view, the first application of the present method is to track the implant insertion thanks to the evolution of the resonance frequencies. The convergence of the resonance frequencies may be determined by predictive methods using numerical simulation. Such approach will allow to decrease the occurrence of unnecessary additional impacts applied when the implant is fully inserted, thus reducing the risk of fractures, while improving the implant primary stability.

A second application concerns the estimation of the insertion length into the femur, which is hardly measurable in clinic. This insertion length is an important criterion defining the end of insertion. By using predictive methods, the correlation between the resonance frequencies and implant displacement into the bone could help to estimate the actual insertion depth.

e. Perspectives and conclusion

Contrarily to previous studies which require modifications of the implant for sensors or shaker fixation, the main advantage of our method is that it does not require any contact with the implant nor bone tissues[16,32,44]. However, it would be relevant in a future study to evaluate respective sensitivity of modes $2Y$ and $2Y_b$ to specific characteristics of the bone-implant interface properties during insertion such as the bone Young's Moduli or the implant positioning in the bone cavity. It would also be interesting to optimize the number and locations of measurement points regarding the shape of the modes of interest identified in this study, in order to make the measurement easier and quicker for the surgeon by calculating only few FRFs on which the resonance frequencies would be identified and used to monitor the femoral stem insertion.

This study investigates the possibility to perform experimental modal analysis directly on the surgical ancillary used to insert uncemented implant into the bone, in order to monitor femoral stem insertion. The results are shown to be consistent with a previously assessed method based on the impact force analysis. The modal parameters of two bending modes of the ancillary in the range [400-8000] Hz are sensitive to the bone-implant contact conditions and a significant correlation was obtained between the variation of the corresponding modal frequencies and the femoral stem displacement into the host bone. This study opens new paths towards the development of noninvasive evaluation methods for the femoral stem insertion monitoring.

7. Acknowledgments

The authors would like to thank Hugues Albini Lomami to assist in preparing specimens and Léa Terriac for help in gathering experimental results.

8. Funding and/or Conflicts of interests/Competing interests

This project has received funding from the European Research Council (ERC) under the European Union's Horizon 2020 research and innovation program, grant agreement No 682001, project ERC (Consolidator Grant 2015 BoneImplant).
There was no conflict of interest for none of the authors.

8. References

1. Albini Lomami, H., C. Damour, G. Rosi, A.-S. Poudrel, A. Dubory, C.-H. Flouzat-Lachaniette, and G. Haiat. Ex vivo estimation of cementless femoral stem stability using an instrumented hammer. *Clinical Biomechanics* 76:105006, 2020.

2. Allemang, R. The modal assurance criterion - Twenty years of use and abuse. *Sound & vibration* 37:14–23, 2003.

3. Alshuhri, A. A., T. P. Holsgrove, A. W. Miles, and J. L. Cunningham. Development of a non-invasive diagnostic technique for acetabular component loosening in total hip replacements. *Medical Engineering & Physics* 37:739–745, 2015.

4. Bosc, R., A. Tijou, G. Rosi, V.-H. Nguyen, J.-P. Meningaud, P. Hernigou, C.-H. Flouzat-Lachaniette, and G. Haiat. Influence of soft tissue in the assessment of the primary fixation of acetabular cup implants using impact analyses. *Clinical Biomechanics* 55:7–13, 2018.

5. Cachão, J. H., M. P. Soares Dos Santos, R. Bernardo, A. Ramos, R. Bader, J. A. F. Ferreira, A. Torres Marques, and J. A. O. Simões. Altering the Course of Technologies to Monitor Loosening States of Endoprosthetic Implants. *Sensors (Basel)* 20:, 2019.

6. Corbett, K. L., E. Losina, A. A. Nti, J. J. Z. Prokopetz, and J. N. Katz. Population-based rates of revision of primary total hip arthroplasty: a systematic review. *PLoS One* 5:e13520, 2010.

7. Dubory, A., G. Rosi, A. Tijou, H. A. Lomami, C.-H. Flouzat-Lachaniette, and G. Haïat. A cadaveric validation of a method based on impact analysis to monitor the femoral stem insertion. *J Mech Behav Biomed Mater* 103:103535, 2019.

8. Eggers, G., M. Rieker, B. Kress, J. Fiebach, H. Dickhaus, and S. Hassfeld. Artefacts in magnetic resonance imaging caused by dental material. *MAGMA* 18:103–111, 2005.

9. Ewins, D. J. Modal testing: theory, practice, and application. Baldock, Hertfordshire, England ; Philadelphia, PA: Research Studies Press, 2000, 562 pp.

10. Fitzgerald, R. H. J., G. W. Brindley, and B. F. Kavanagh. The Uncemented Total Hip Arthroplasty: Intraoperative Femoral Fractures. *Clinical Orthopaedics and Related Research*® 235:61–66, 1988.

11. Georgiou, A. P., and J. L. Cunningham. Accurate diagnosis of hip prosthesis loosening using a vibrational technique. *Clinical Biomechanics* 16:315–323, 2001.

12. Goossens, Q., S. Leuridan, P. Henyš, J. Roosen, L. Pastrav, M. Mulier, W. Desmet, K. Denis, and J. Vander Sloten. Development of an acoustic measurement protocol to monitor acetabular implant fixation in cementless total hip Arthroplasty: A preliminary study. *Medical Engineering & Physics* 49:28–38, 2017.

13. Goossens, Q., L. Pastrav, J. Roosen, M. Mulier, W. Desmet, J. Vander Sloten, and K. Denis. Acoustic Analysis to Monitor Implant Seating and Early Detect Fractures in Cementless Tha: An in Vivo Study. *J. Orthop. Res.* , 2020.doi:10.1002/jor.24837

14. Hailer, N. P., G. Garellick, and J. Kärrholm. Uncemented and cemented primary total hip arthroplasty in the Swedish Hip Arthroplasty Register. *Acta Orthop* 81:34–41, 2010.

15. Henyš, P., and L. Čapek. Material model of pelvic bone based on modal analysis: a study on the composite bone. *Biomech Model Mechanobiol* 16:363–373, 2017.

16. Henyš, P., and L. Čapek. Impact Force, Polar Gap and Modal Parameters Predict Acetabular Cup Fixation: A Study on a Composite Bone. *Ann Biomed Eng* 46:590–604, 2018.

17. Henys, P., L. Capek, J. Fencl, and E. Prochazka. Evaluation of acetabular cup initial fixation by using resonance frequency principle. *Proc Inst Mech Eng H* 229:3–8, 2015.

18. Henyš, P., S. Leuridan, Q. Goossens, M. Mulier, L. Pastrav, W. Desmet, J. V. Sloten, K. Denis, and L. Čapek. Modal frequency and shape curvature as a measure of implant fixation: A computer study on the acetabular cup. *Medical Engineering & Physics* 60:30–38, 2018.

19. Hériveaux, Y., V.-H. Nguyen, D. Geiger, and G. Haiat. Elastography of the bone-implant interface. *Scientific Reports* 9:, 2019.

20. Khanuja, H. S., J. J. Vakil, M. S. Goddard, and M. A. Mont. Cementless Femoral Fixation in Total Hip Arthroplasty. *Journal of Bone and Joint Surgery* 93:500–509, 2011.

21. Kikuchi, S., K. Mikami, D. Nakashima, T. Kitamura, N. Hasegawa, M. Nishikino, A. Kanaji, M. Nakamura, and T. Nagura. Laser Resonance Frequency Analysis: A Novel Measurement Approach to Evaluate Acetabular Cup Stability During Surgery. *Sensors (Basel)* 19:, 2019.

22. Kim, Y. Y., J.-C. Hong, and N.-Y. Lee. FREQUENCY RESPONSE FUNCTION ESTIMATION VIA A ROBUST WAVELET DE-NOISING METHOD. *Journal of Sound and Vibration* 244:635–649, 2001.

23. Kurtz, S. M., E. Lau, K. Ong, K. Zhao, M. Kelly, and K. J. Bozic. Future Young Patient Demand for Primary and Revision Joint Replacement: National Projections from 2010 to 2030. *Clin Orthop Relat Res* 467:2606–2612, 2009.

24. Lannocca, M., E. Varini, A. Cappello, L. Cristofolini, and E. Bialoblocka. Intra-operative evaluation of cementless hip implant stability: A prototype device based on vibration analysis. *Medical Engineering & Physics* 29:886–894, 2007.

25. Leuridan, S., Q. Goossens, L. Pastrav, J. Roosen, M. Mulier, K. Denis, W.

Desmet, and J. V. Sloten. Determination of replicate composite bone material properties using modal analysis. *J Mech Behav Biomed Mater* 66:12–18, 2017.

26. Mathieu, V., A. Michel, C.-H. Flouzat Lachaniette, A. Poignard, P. Hernigou, J. Allain, and G. Haïat. Variation of the impact duration during the in vitro insertion of acetabular cup implants. *Medical Engineering & Physics* 35:1558–1563, 2013.

27. Michel, A., R. Bosc, J.-P. Meningaud, P. Hernigou, and G. Haiat. Assessing the Acetabular Cup Implant Primary Stability by Impact Analyses: A Cadaveric Study. *PLoS ONE* 11:e0166778, 2016.

28. Michel, A., V.-H. Nguyen, R. Bosc, R. Vayron, P. Hernigou, S. Naili, and G. Haiat. Finite element model of the impaction of a press-fitted acetabular cup. *Med Biol Eng Comput* 55:781–791, 2017.

29. Mohammed Rafiq Abdul-Kadir, U. Hansen, and R. Klabunde. Finite element modelling of primary hip stem stability: The effect of interference fit - ScienceDirectat <https://www.sciencedirect.com/science/article/pii/S0021929007004381>

30. Morohashi, I., H. Iwase, A. Kanda, T. Sato, Y. Homma, A. Mogami, O. Obayashi, and K. Kaneko. Acoustic pattern evaluation during cementless hip arthroplasty surgery may be a new method for predicting complications. *SICOT J* 3:, 2017.

31. Nakashima, D., K. Ishii, M. Matsumoto, M. Nakamura, and T. Nagura. A study on the use of the Osstell apparatus to evaluate pedicle screw stability: An in-vitro study using micro-CT. , 2018.at <https://journals.plos.org/plosone/article?id=10.1371/journal.pone.0199362>

32. Pastrav, L. C., S. V. N. Jaecques, M. Mulier, and G. Van Der Perre. Detection of the insertion end point of cementless hip prostheses using the comparison between successive frequency response functions. *J Appl Biomater Biomech* 6:23–29, 2008.

33. Pérez, M. A., and B. Seral-García. A finite element analysis of the vibration behaviour of a cementless hip system. *Comput Methods Biomech Biomed Engin* 16:1022–1031, 2013.

34. Pilliar, R. M., J. M. Lee, and C. Maniatopoulos. Observations on the effect of movement on bone ingrowth into porous-surfaced implants. *Clin. Orthop. Relat. Res.* 108–113, 1986.

35. Pivec, R., A. J. Johnson, S. C. Mears, and M. A. Mont. Hip arthroplasty. *Lancet* 380:1768–1777, 2012.

36. Qi, G., W. P. Mouchon, and T. E. Tan. How much can a vibrational diagnostic tool reveal in total hip arthroplasty loosening? *Clin Biomech (Bristol, Avon)* 18:444–458, 2003.

37. Richardson, M. H., and D. L. Formenti. Parameter Estimation from Frequency Response Measurements using Rational Fraction Polynomials. 15, 1982.

38. Schmalzried, T. P., L. M. Kwong, M. Jasty, R. C. Sedlacek, T. C. Haire, D. O. O'Connor, C. R. Bragdon, J. M. Kabo, A. J. Malcolm, and W. H. Harris. The mechanism of loosening of cemented acetabular components in total hip arthroplasty. Analysis of specimens retrieved at autopsy. *Clin Orthop Relat Res* 60–78, 1992.

39. Sloan, M., A. Premkumar, and N. P. Sheth. Projected Volume of Primary Total Joint Arthroplasty in the U.S., 2014 to 2030. *J Bone Joint Surg Am* 100:1455–1460, 2018.

40. Tijou, A., G. Rosi, R. Vayron, H. A. Lomami, P. Hernigou, C.-H. Flouzat-Lachaniette, and G. Haïat. Monitoring cementless femoral stem insertion by impact analyses: An in vitro study. *Journal of the Mechanical Behavior of Biomedical Materials* 88:102–108, 2018.

41. Ulrich, S. D., T. M. Seyler, D. Bennett, R. E. Delanois, K. J. Saleh, I. Thongtrangan, M. Kuskowski, E. Y. Cheng, P. F. Sharkey, J. Parvizi, J. B. Stiehl, and M. A. Mont. Total hip arthroplasties: What are the reasons for revision? *Int Orthop* 32:597–604, 2008.

42. Whitwell, G., C. L. Brockett, S. Young, M. Stone, and T. D. Stewart. Spectral analysis of the sound produced during femoral broaching and implant insertion in uncemented total hip arthroplasty. *Proc Inst Mech Eng H* 227:175–180, 2013.

43. Wong, A. S., A. M. R. New, A. Ritchie, and M. Taylor. Influence of an Interference-fit on the strain distribution in the implanted proximal femur. 3.

44. Yousefsani, S. A., H. Dejnabadi, O. Guyen, and K. Aminian. A Vibrational Technique for In Vitro Intraoperative Prosthesis Fixation Monitoring. *IEEE Trans Biomed Eng* 67:2953–2964, 2020.

SUPPLEMENTARY DATA

Appendix A

A.1 Instrumented hammer and signal processing

The variation of the force as a function of time was recorded with the dynamic piezoelectric sensor (208C05, PCB Piezoelectronics, Depew, New York, USA). A dedicated data acquisition module (NI 9234, National Instruments, Austin, TX, USA) with a sampling frequency of 51.2 kHz and a resolution of 24 bits was linked to a LabView interface (National Instruments, Austin, TX, USA) to record $s_i(t)$ for a duration of 13 ms.

The same signal processing method as the one developed in Tijou et al[40] was employed in order to analyze the insertion force signal $s_i(t)$ applied with the instrumented hammer (1) on the top of the ancillary. An indicator, noted D_i was calculated for each impact #*i*. The indicator D_i, given in ms, corresponds to the time difference between the time of the second and the first local maxima of the signal $s_i(t)$ and is calculated as follows:

$$D_i = f_2(s_i(t)) - f_1(s_i(t)) \quad (5)$$

where the functions f_1 and f_2 are applied to the signal $s_i(t)$ and are defined as the time of the maximum value of the first and second peak of the signal, respectively.

A.2 Video Analysis

The distance of interest, denoted E_i (in mm), corresponds to the relative displacement of the ancillary with respect to the bone phantom at insertion step #*i* compared to its initial position and is calculated as follow:

$$E_i = e_0 - e_i \quad (6)$$

where e_0 and e_i are the distances between marker #M_1 and #M_2 at the beginning of the insertion procedure and at the insertion step #*i*, respectively (see Fig. 1). The

distance between the marker #M_1 glued on the ancillary and the marker #M_3, glued on the stem remains constant throughout the insertion procedure and is used as a scale to convert pixels into metric distance.

A.3 Reproducibility of EMA

The measurement protocol described in Fig. 1 and the corresponding signal processing were repeated 3 times at each insertion step #*i* during the implant insertion in bone phantom specimen #*3*, which was chosen arbitrarily. The mode detection and modal frequency values f^n determined with the modal analysis using the RFP method for the frequency range [400-8000] Hz were compared for each insertion step #*i.* The same modes were detected for the two analysis performed at each insertion step and the averaged difference between the modal frequencies f^n obtained for the three analysis over the all insertion procedure was smaller than the software resolution, which is equal to 4 Hz. This result validates the correctness of the RFP method to determine all resonance frequencies in this study.

A.4 Responses measured by instrumented hammer

An example of several force signals $s_i(t)$ obtained for different impacts during the FS insertion in a given specimen (bone phantom specimen #*3*) is presented in Fig. 8. Each impact corresponds to a specific insertion step #*i* indicated above each second peak of the force signal. The value of the indicator D_i first decreases with the insertion step #*i* and then stays constant after eight impacts. These results are in agreement with the results found in Tijou et al[40].

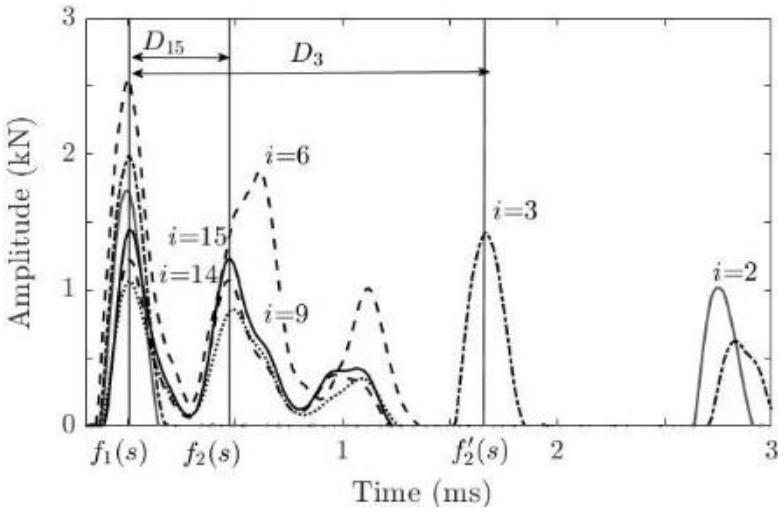

Figure 8 Illustration of different signals $s_i(t)$ corresponding to the variation of the force applied to the ancillary to insert the femoral stem as a function of time for different impact number #i. Data obtained with bone phantom specimen #3.